Spectroscopic investigation of substrates contaminated by Chemical Warfare Agents

Journal:	*Journal of Analytical Atomic Spectrometry*
Manuscript ID	JA-ART-08-2015-000333.R1
Article Type:	Paper
Date Submitted by the Author:	12-Oct-2015

Complete List of Authors:	Landström, Lars; Swedish Defence Research Agency, FOI, CBRN Defence and Security Örebrand, Lillemor; Swedish Defence Research Agency, FOI, CBRN Defence and Security Svensson, Kristoffer; Swedish Defence Research Agency, FOI, CBRN Defence and Security Andersson, Per Ola; Swedish Defence Research Agency, FOI, CBRN Defence and Security

Spectroscopic investigation of substrates contaminated by Chemical Warfare Agents

Lars Landström,* Lillemor Örebrand, Kristoffer Svensson, and Per Ola Andersson

CBRN Defence and Security, Swedish Defence Research Agency (FOI), SE-901 82 Umeå, Sweden

Abstract

Laser induced breakdown spectroscopy (LIBS) and Attenuated Total Reflection Fourier Transform Infrared (ATR-FTIR) spectroscopy have been evaluated for the purpose of analyzing contaminated and decontaminated susbtrates, such as Si wafers and different Chemical Agent Resistant Coating (CARC) paint systems. As contaminants, sarin (GB) and soman (GD) were studied as well as two simulant organophosphate compounds, trimethyl phosphate (TMP) and tributyl phosphate (TBP). First, the clean substrates were analyzed to obtain reference spectra and to reveal any interfering spectral overlap. Phosphorous lines were used to indirectly follow the occurence of organophosphates via LIBS, which was also utilized for depth profile analysis into the substrates. Infrared absorption spectroscopy was also applied as a tool to monitor any residual contaminants. As expected, results showed that no, or below the detection limit, diffusion of the contaminants occured into Si or the CARC paints. However, on top of and within a simple cover paint it was possible to detect P emission lines by LIBS, and ATR-FTIR revealed the presence of, e.g., C-O-P, P-F, and P=O vibrational bands, indicating GB and GD and/or breakdown products. The LIBS technique also showed promising results for monitoring diffusion processes within one paint matrix. Rinse and elution steps performed on the non-CARC paint had little effect as decontamination procedures.

I. INTRODUCTION

To evaluate and possibly improve decontamination procedures with the purpose of removing/destroying hazardous substances such as Chemical Warfare Agents (CWA) and Toxic Industrial Chemicals (TIC) demands a deep knowledge and understanding of a wide range of physical and chemical processes, as well as analytical and theoretical tools to follow and predict such processes[1–4]. Among these areas are the detection of the substance(s) on various substrates and matrices, preferably both before and after the decontamination. If the detection technique also allows for probing within certain substrates it may also be possible to monitor, e.g., diffusion and penetration of certain chemicals (or elements)[5]. A variety of techiques are available for the detection of CWA and TIC, see ref.[4] and references therein, and methods are also being developed for depth profiling purposes[6]. In the present report we investigate two spectroscopic techniques, namely Laser Induced Breakdown Spectroscopy (LIBS) and Attenuated Total Reflection Fourier Transform Infrared (ATR-FTIR) spectroscopy and their possibilities within surface detection (for residual organophosphates after evaporation). In addition, as LIBS can be used for depth profiling[7,8], any diffusion of the chemicals into the substrates was also studied. Systems utilizing these techniques can be made man portable and as they commonly allow for fast operation, it may open up for rapid in-field applications related to contamination and decontamination issues useful for, e.g., first responders and military personnel.

LIBS is an atomic emission spectroscopy technique where a high intensity laser pulse initiates a plasma and an optical detection system is used to analyze the emitted, characteristic elemental (and/or molecular fragment) light. Common experimental set-ups and in-depth theoretical background can be found in refs.[9–15]. LIBS is usually denoted as a quasi non-destructive analytic technique, as only a small volume is ablated and analyzed, and is also a common method for applications related to rapid ”real time” elemental and compositional analysis of various materials[16–19]. It has also proven to be useful in other, more specific, applications aiming towards CWA and Biological Warfare Agents (BWA) detection and early warning[9,20–26]. Furthermore, results concerning LIBS in connection to detection and identification of different explosives[27,28] and also radiological (RN) materials[29] can be found in the literature. Unfortunately, when considering the classic CWA, the indicative elements (e.g., P, F, Cl and S) are high ionization elements, thus being more challenging to monitor than, e.g., metals such as Al, Ca, Mg and Na. Furthermore, the matrix effect will also pose a challenge when analyzing different materials (matrices) with the purpose of

evaluating the effect of different decontamination procedures.

ATR-FTIR is widely used for rapid and easy identification of unknown samples, and also to monitor changes of specific molecular vibrational modes upon chemical reactions or interactions[30]. Similar to LIBS it is executed by direct measurements on the surfaces without need for any sample preparation, however, part of the measuring system, the internal reflection element/crystal, needs to be in contact with the sample, as the IR radiation is totally reflected within the internal reflection element (IRE) at the interface to the surrounding medium (sample). The evanescent field, which decays exponentially from this interface, probes IR active modes within, typically, a few microns range.

In the present report, the contamination of a few organophosphates on different substrates were studied, indirectly by LIBS, via monitoring the intensity of P emission line(s), and also by ATR-FTIR by measurements on the contaminated and decontaminated surfaces as well as the pure analytes and substrates. No sample preparation was performed before the spectroscopic studies and the overall purpose was to evaluate the techniques for applications such as: detection of contamination on and within the substrate and the efficiency of different decontamination procedures. It is noted that detection of phosphorous by means of LIBS has earlier been performed in a variety of matrices, e.g., minerals[18,31], pharmaceutical products[32], and steel[33], and that ATR-FTIR studies have been conducted on CWA and related chemicals[34].

As model systems in this study, Si wafers and two different paint systems contaminated by simulant chemicals and neat CWA were used. The motivation was to show a proof-of-concept for using the spectroscopic techniques for the above specified applications, however, with no emphasis on detection limits. The paint systems were chosen as several questions and problems related to, e.g., protection, contamination and decontamination for these systems can be found[4,6,35].

II. EXPERIMENTAL

To induce the breakdown plasma, a pulsed tunable laser system with the laser light focused onto the samples with an angle of incidence of about 30° was used. The laser wavelength was set to 264 nm to ensure absorption of a wide range of materials and to initiate effective ablation at the low pulse energies available. In addition, this wavelength is close to cheaper (non-tunable) laser systems, like frequency quadrupled Nd:YAG and Nd:YLF laser sources. A repetition rate of 10 Hz and a pulse energy of about 2 mJ with pulse duration of $\sim$10 ns was used for all experiments.

Rates of ablation for a paint system were determined by measuring the depth of the ablated crater by light optical microscopy for different number of laser pulses. The area of the ablated spot was $\sim$0.05 mm^2 and the emitted light from the laser induced plasma was imaged onto a round to slit optical fiber bundle (48$\times$50 μm diameter fibers) coupled into a $f = 500$ mm Czerny-Turner type spectrograph, equipped with a 2400/mm grating and an intensified CCD detector (DH720I-18F-03 from Andor). The physical slit on the spectrograph entrance was set to $\sim$10 μm. To ensure that most of the shortlived phosphorous lines were collected, a very short delay was used (about 10 ns after the laser pulse) and the light was collected during a gate pulse of 2 μs. Even though a strong Stark broadening was observed, good signal to noise levels were achieved at UV wavelengths whilst monitoring the P lines from a pressed pellet of sodium phosphate. Saturation of the detector was avoided by setting proper gain. When calculating the peak intensity from the single shot LIBS spectra, a normalization to the total intensity in the wavelength window monitored was applied to reduce the effect of pulse to pulse variation in, e.g., energy.

The application of LIBS to measure any organophosphate contamination was investigated on three different surfaces; Si wafer and two different Chemical Agent Resistant Coating (CARC) paint systems on aluminum plates. One paint system (A) consisted of a CARC paint applied directly onto the aluminum plate and subsequently painted with a cover paint and in the second paint system (B), a primer paint was applied on the Al plate and subsequently coated with a CARC paint.

Organophosphates used were; trimethyl phosphate (TMP), tributyl phosphate (TBP), sarin (GB), and soman (GD). Purity of the live agents was determined to > 98% by Nuclear Magnetic Resonance (NMR). Typically, 5 μl droplets of the different organophosphates were deposited onto the different substrate surfaces and left in a fume hood to evaporate, to leave residues, and/or diffuse into the substrates. All experiments were performed at standard laboratory conditions. Paint system A was analyzed in most detail, where the neat CWA contaminated substrates were measured after i) evaporation, ii) a rudimentary decontamination procedure (rinse by 50 ml 96% ethanol), and iii) after an elution step. The elution was performed at room temperature during 4 hours on a rocking table where each sample was immersed in a 50 ml 9:1 mixture of hexane and acetone spiked with undecane as internal standard for GC-MS analysis. The other substrates were only analyzed after evaporation of the simulants and CWA.

Furthermore, ATR-FTIR analysis was performed on live agents and on CWA contaminated paint system A. Reference spectra were obtained from the neat agents as well as from clean paint

system A surfaces. Measurements on contaminated A substrates were performed after the rudimentary ethanol decontamination described above. All infrared spectra were recorded between 600 and 4000 cm^{-1} with a spectral resolution of 4 cm^{-1}. A single reflection ZnSe crystal ($d \approx 5$ mm for the active area) was used for all experiments.

III. RESULTS AND DISCUSSION

A. Clean surfaces

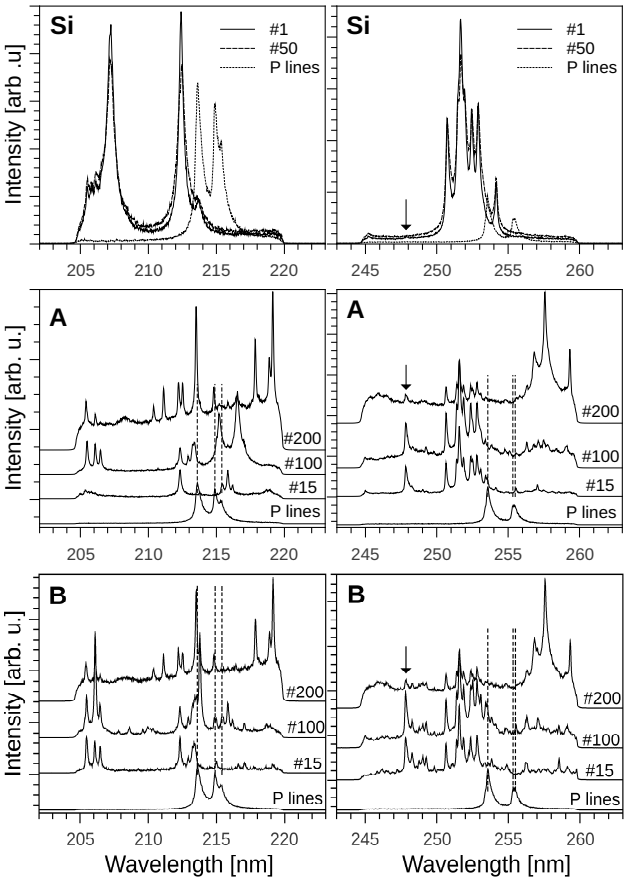

FIG. 1: LIBS spectra from the clean substrates (Si wafer, A and B paint systems) and phosphorous lines (from ablation of a sodium phosphate pellet). The two wavelength regions of interest are displayed. The different numbers refer to different laser pulses (depths). The spectra in the four lower graphs are shifted in y for clarity and the arrow in the right panel graphs indicates the position of the 247.9 nm carbon emission line. In addition, the position of the P lines are indicated by vertical dashed lines.

As mentioned earlier, LIBS can be challenging for the purpose of detecting certain elements in

a complex matrix, mainly due to the occurrence of interfering/overlapping elemental lines. With the experimental parameters used here, this overlap can be expected to be even more problematic because of the Stark broadened peaks. However, for this particular investigation we chose to set short delay times in order to collect the majority of the P emission. Furthermore, the relatively poor (for atomic emission spectroscopy purposes) spectral resolution of the system at UV wavelengths also sets a limit for differentiating between nearby elemental lines.

First, spectra from clean surfaces and sodium phosphate pellets were acquired to investigate any interfering lines. The LIBS system could be operated with acceptable optical losses in the UV-VIS region, and the strongest phosphorus lines are then found at 213.6, 214.9, 215.4, 253.6, 255.3, and 255.5 nm, respectively[36]. Moreover, carbon has a strong emission line at 247.9 nm and will be accessible while monitoring the P lines around 255 nm. To be able to analyze the strong P lines with the spectrograph used, two different wavelength windows, 205-220 and 245-260 nm, were studied and the results are depicted in Figure 1.

The two top graphs in Figure 1 (Si) show spectra from the first laser pulse (#1) and 50th laser pulse (#50) to illustrate the slight differences in spectra acquired by single shot LIBS. Fluctuations in laser pulse energy and ablated area properties will inevitably produce variations in acquired spectra. Furthermore, the native $\sim$2 nm oxide layer may also influence the LIBS spectrum obtained by the first pulse. Strong Si peaks are observed at, e.g., 207.2, 212.4, 213.7 nm (left upper graph) and also the lines in the 250.7-253.2 nm range (right upper graph)[36]. The emission line at 254.2 nm is unassigned but will be briefly discussed later in subsection III B. As an example of the surface sensitivity of the method, a small peak could be observed at 247.9 nm (C line) for the first pulse, most likely originating from surface contamination from ambient air onto the Si wafer. The paint systems consisted of two different paints on top of an aluminum plate, resulting in a three layered sandwich system (see also Figure 2). The three different spectra shown in the graphs are representative single shot spectra from each of these regions and are illustrated in the plots as laser shots #15, #100, and #200.

Obviously, overlapping lines occur between many of the substrates and P lines at the wavelength regions of interest, see Figure 1. Paint system A appears to have the least overlap with the P lines. For carbon detection at 247.9 nm (see arrows in Figure 1), it only looks promising for the Si wafer, as the spectra from the different paints already exhibit a quite strong peak, likely originating from the carbon containing binders in the paint.

To illustrate the depth profiling possibilities of LIBS for the experimental system and settings

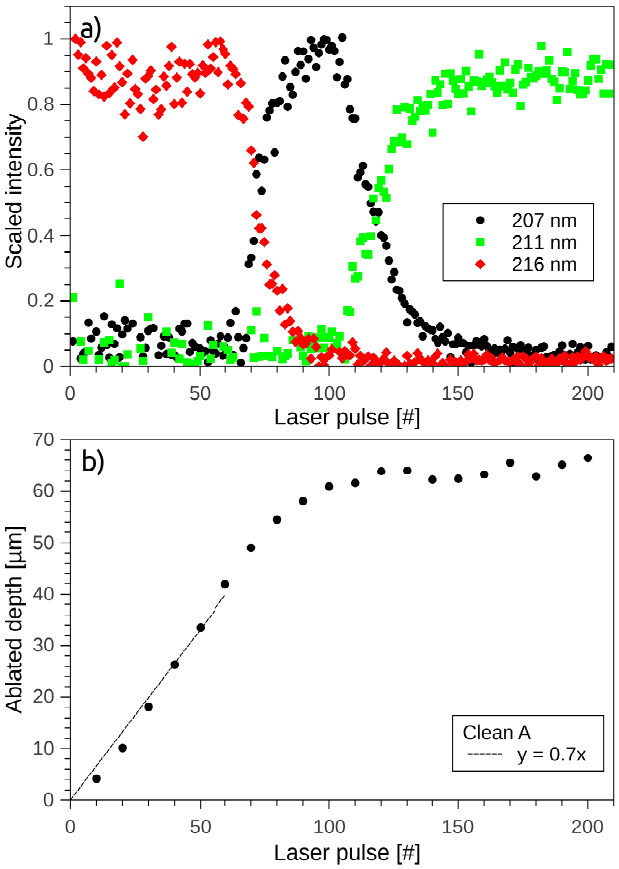

FIG. 2: a) Intensity of three different emission lines as function of laser pulse, obtained from a clean paint system A substrate. Intensities were scaled to the highest value. b) Ablated depth for paint system A as observed by light optical microscopy at different number of laser pulses.

used here, the intensity of three different (unassigned) emission lines as function of number of laser pulses, is shown in Figure 2a. As can be seen, the three different regions (cover paint, CARC and aluminum plate) can be differentiated. However, no sharp transitions are observed at the two interfaces inside the sandwich structure, resulting in that ”pure” LIBS spectra from the cover paint can be obtained up to laser pulse ∼60 and the ”pure” CARC is only observed in approximately the #90-#110 laser pulse range. This effect can be related to, e.g., i) inhomogeneous/uneven interface, ii) laser spot energy distribution, iii) thermal diffusion effects, and iv) laser angle of incidence.

The ablation rate for paint system A was measured to be approximately 0.7 μm/pulse for the first ∼60 pulses, see Figure 2b. This experimentally obtained rate of ablation was used to transfer the number of laser pulses into depth domain.

B. Simulant chemicals trimethyl phosphate (TMP) and tributyl phosphate (TBP)

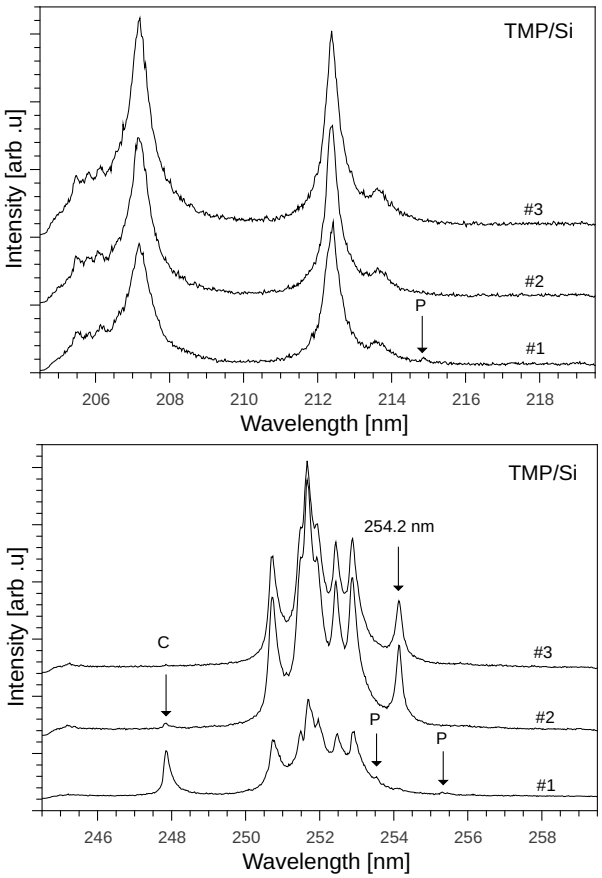

FIG. 3: Single shot LIBS spectra (two different wavelength windows) from the three first laser pulses (#1-3) on a stain from TMP on a Si wafer. Note the 254.2 nm line occuring after the first pulse.

Differences in wetting, adsorption and evaporation could be observed when 5 μl droplets of the two simulant chemicals were applied onto the different surfaces. On polished, but otherwise untreated Si wafers, both TMP and TBP formed $\sim$10 mm in diameter droplets and the TMP droplets evaporated, leaving only a small stain, after about 24 hours. TBP, however, was still in liquid form after more than four weeks. On the B paint system surface with the CARC paint as the topmost layer, TBP rapidly spreads to an area of about 10 cm^2 whereas TMP formed similar droplets as on Si. TMP was fully evaporated after about 24 h at normal temperature and pressure. No visible stain was observed by the naked eye. TBP needed longer time, more than 48 hours, to evaporate which is likely related to its lower vapor pressure. For TBP, a slight discoloration could be observed where the liquid had been. On paint system A, both simulant chemicals rapidly spread to about 10 cm^2 and no liquid layer could be observed after 24 hours, however, stains/discoloration

from the droplets were easily distinguishable by the naked eye. The differences in evaporation time of TBP between Si and the paint systems can be explained by the smaller surface to volume ratio of the droplets on the wafer, resulting in a lower rate of evaporation.

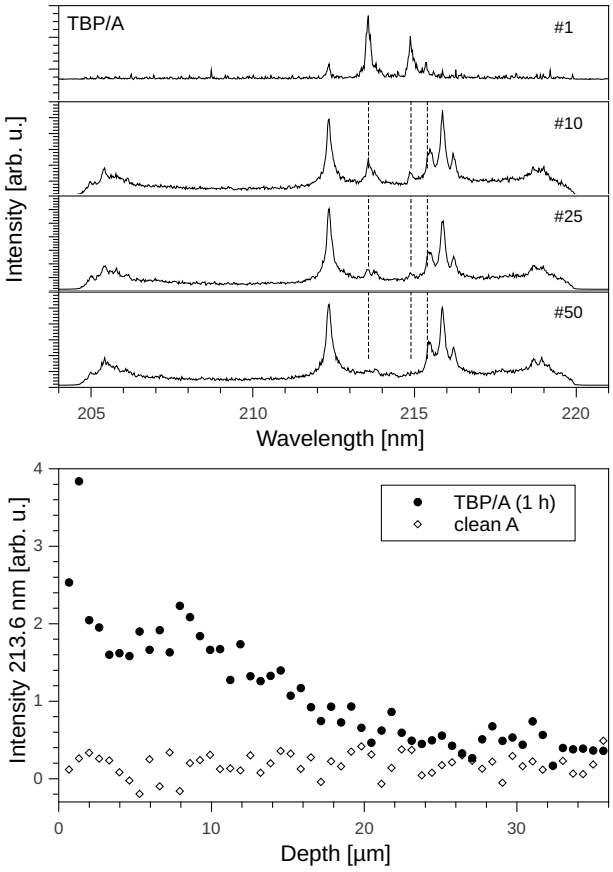

FIG. 4: The upper panels show single shot LIBS spectra from TBP contaminated cover paint A (after one hour) for different laser pulses. The position of P emission lines are indicated by dashed vertical lines in three of the graphs. Lower graph depicts the intensity of the P (213.6 nm) peak as function of depth where the peak intensity was normalized to the total intensity in the wavelength window.

Typical optical emission spectra from plasma induced by the first three laser pulses are shown in Figure 3, where the laser was focused onto the stain observed on the Si wafer after TMP evaporation. In three of the graphs, the position of the P lines at 214.9, 253.6 and 255.3 nm, respectively, are indicated. Apparently, only weak P peaks, relative bulk material emission lines, could be observed for the first laser pulse. The most notable differences were observed at the wavelength window centered around 252 nm (lower graph in Figure 3), where the C peak at 247.9 nm is clearly seen for the first and second laser shot. However, a small C peak was also observed for

the first shot on ”clean” Si wafer (see Figure 1), but the relatively strong peak seen here suggests that it originates from remaining TMP residues. In addition, an unassigned peak at 254.2 nm is not present in the first shot spectra (was present in the first shot clean Si spectrum, see Figure 1) and the relative intensity of the Si peaks in the 250.7-252.9 nm range is lower compared to spectra #2 and #3, suggesting that the amount (depth) of Si ablation is lower in this case, as the removal of material from the stain results in less laser pulse energy to ablate Si. Morever, the stain may modifiy the optical properties, thus affecting the ablation. The native oxide layer may also affect the first pulse, however, the 254.2 nm peak could be observed for the first laser pulse on the clean surface, see Figure 1, and similar Si line intensities were observed for the first and second laser pulse. The 254.2 nm peak can most likely be attributed to Fe as it is known to be one of the most common contaminants in Si wafers[37]. Possibly, the majority of Si removed during this first pulse originates from the ∼2 nm native oxide layer and not from the bulk Si wafer.

Similar to the Si wafers, it was difficult to detect any P lines on the B paint system after the simulant chemicals evaporated. Only low intensity P lines were sometimes found for the first laser pulse (spectra not shown).

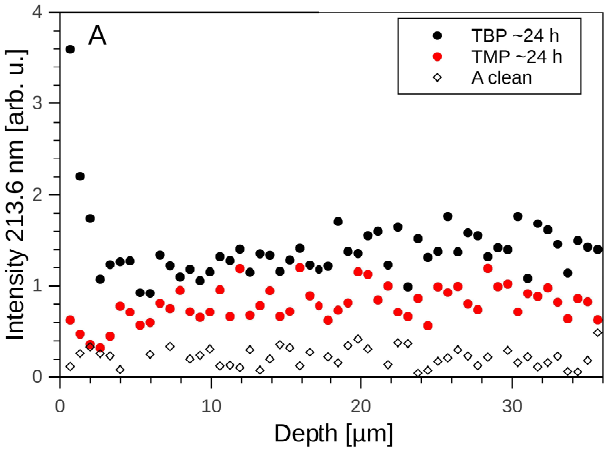

FIG. 5: Intensity of the P (213.6 nm) emission line as function of depth (normalized to total intensity). Paint system A contaminated by TBP and TMP and measurements performed 24 hours after droplet deposition.

LIBS spectra taken from the area where TBP has been deposited on the paint system A are shown in Figure 4 (upper panels) together with the intensity of the 213.6 nm P peak during depth profiling (lowest panel). Here, the spectra were acquired about one hour after the droplet was deposited. At that time, the liquid had not fully evaporated, i.e., a damp spot could still be observed. The spectra and line intensities were, in the case shown in Figure 4, taken outside the obvious

wet spot but still within the area where TBP had been deposited. The spectrum obtained by the first laser pulse (#1 in Figure 4) was dominated by the P lines and the intensity of the peaks were relatively low. Likely, there were still a large portion of liquid phase TBP in the topmost surface layer resulting in poor plasma formation for the experimental parameters used. As the number of laser pulses increased above ∼10, the intensity of P lines decreased indicating that TBP was diffusing into the cover paint. Indeed, after ∼24 hours, the intensity of the 213.6 nm P line was roughly constant throughout most of the cover paint, see Figure 5.

Weaker P emission lines were measured for TMP relative TBP, see Figure 5. This difference indicates that a lower concentration of TMP penetrates into the topmost paint layer. Even though the TMP molecule is smaller than TBP, and thus likely to exhibit a larger mobility, we attriubte the observed difference to the vapor pressures of the two liquids. As TMP evaporates much faster than TBP, it will limit the amount accessible to contaminate and diffuse into the cover paint.

No P lines were observed in the CARC layer for the A paint system (spectra not shown). Here, some interfering lines complicate the identification of weak P emission lines, however, similar P line intensities as in the top-most paint layer (see, e.g., pulse #10 in Figure 4) would most likely be distinguishable in the spectra.

C. Nerve agents sarin (GB) and soman (GD) on paint system A

In general, the analysis of substrates contaminated by the two CWA showed a similar behavior as for the simulants (i.e,. only small stains could sometimes be observed after evaporation on Si and paint system B). Therefore, only results obtained from paint system A are shown and discussed here, including the effect of decontamination steps, e.g., ethanol rinse and elution to gain further insight about agent/substrate interactions and also to evaluate the efficiency.

The intensity of the 213.6 nm P line as function of depth, at different times after deposition, as well as after rinse and elution is shown in Figure 6. Similar as for the two simulant chemicals, a gradient was observed as the CWA were drying in and evaporating (45 min. and 1 h in the graphs, respectively), again suggesting that the technique might be suitable for monitoring the dynamics of diffusion to some extent. After one day, a more even distribution was found inside the cover paint for GB, whereas a gradient was still observed for GD (see Figure 6), i.e., GB diffuses faster than GD into the paint. These results indicate differences in mobility of the two CWA within the cover paint, probably due to GB being a slightly smaller molecule than GD and that there may

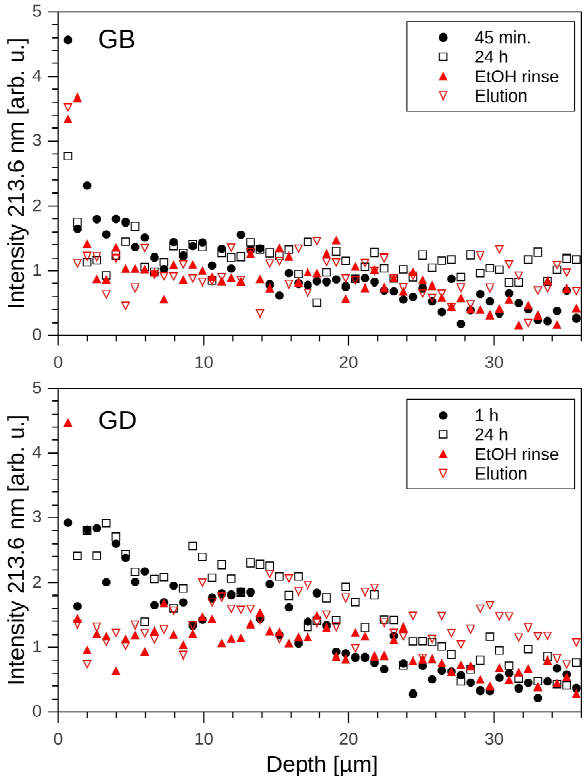

FIG. 6: Normailzed intensity of the P (213.6 nm) emission line is plotted as function of depth for paint system A contaminated by GB and GD after different times and treatments. (The average normalized signal at 213.6 nm of clean paint was 0.2.)

also exist differences in molecule/substrate interactions such as the strengths of physisorption and chemisorption. Further studies are needed to clarify the observed difference.

A simple rinse with ethanol only resulted in minor changes in the measured P line intensities, see Figure 6, and in terms of decontamination, the four hour elution does not seem to affect the agents inside the paint much either. Subsequent analysis by GC-MS on the eluate revealed that ∼0.5% of the initially applied amount was found for both agents. As the decotamination procedures were performed more than three days after the droplets were applied, a different intensity distribution could be observed through the cover paint. In addition, leaving the samples soaked in the eluate for 4 hours (and the subsequent drying) may also affect the distribution of the contaminants within the substrate.

Analysis was as also performed by ATR-FTIR spectroscopy on contaminated and ethanol rinsed paint system A to extract information about any residual contamination and possibly also interactions between the contaminant and substrate. Reference spectra of sarin, soman, and clean

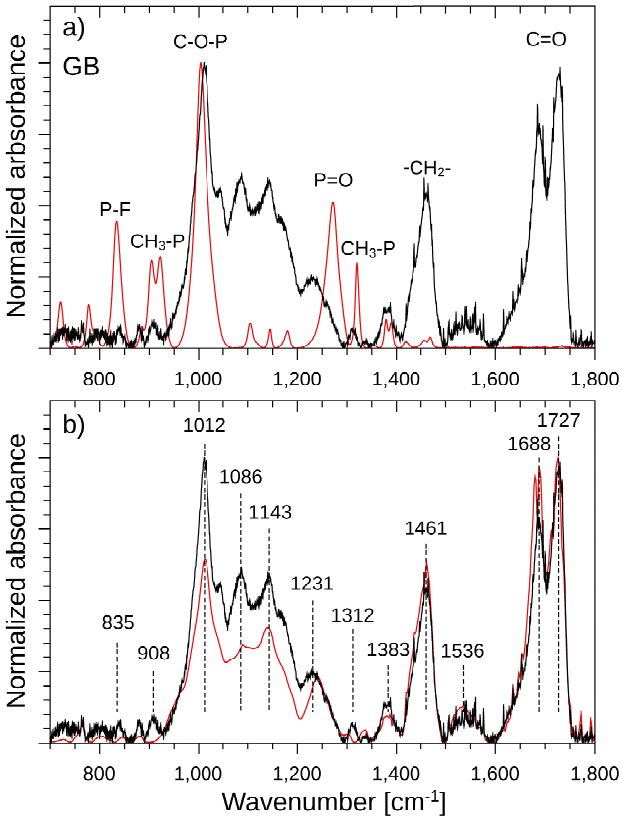

FIG. 7: Normalized ATR-FTIR spectra. The black spectrum in a) and b) is the same, namely from sarin contaminated paint system A. The red spectrum in a) originates from neat sarin liquid and the red one in b) corresponds to clean paint system A.

paint system A are shown in Figures 7 and 8 together with representative spectra from contaminated and ethanol rinsed surfaces. Here, only the fingerprint region is considered. Higher frequency modes, corresponding to C-H vibrations, can be found in the supplementary information (Figure S1) together with peak assignments (see Table S1).

When looking at the pure G agents (GB and GD), they show, as expected, spectral similarities. The most pronounced peaks for sarin (Figure 7a and S1) are located at (and assigned to): 835 (ν(P-F)), 905 and 922 (ρ_{as}(CH_3-P)), 1004 (ν_{as}(C-O-P)), 1272 (ν_s(P=O)) and 1320 cm^{-1} (δ_s(CH_3-P)). In addition to these, soman exhibits a sharp peak at 998 cm^{-1} (Figure 8a) and is attributed to δ_s(C-C-C)[38]. In general, the peak positions are in good agreement with reported literature data[34,38–40] (including the C-H frequencies[34,38,39]).

Similar to LIBS spectra, the background (matrix/substrate) signal may be a complicating issue also for ATR-FTIR analysis. Apparently, a majority of the bands from the substrate overlaps with

those originating from the G agents analyzed here, see Figures 7 and 8, with the exception of the peaks close to 1700 cm^{-1}, which are well separated from CWA bands and ascribed to C=O stretching. No further assignment of the substrate peaks is done here, but FTIR analysis of paint systems comprising different types of pigments have been documented earlier[41–43].

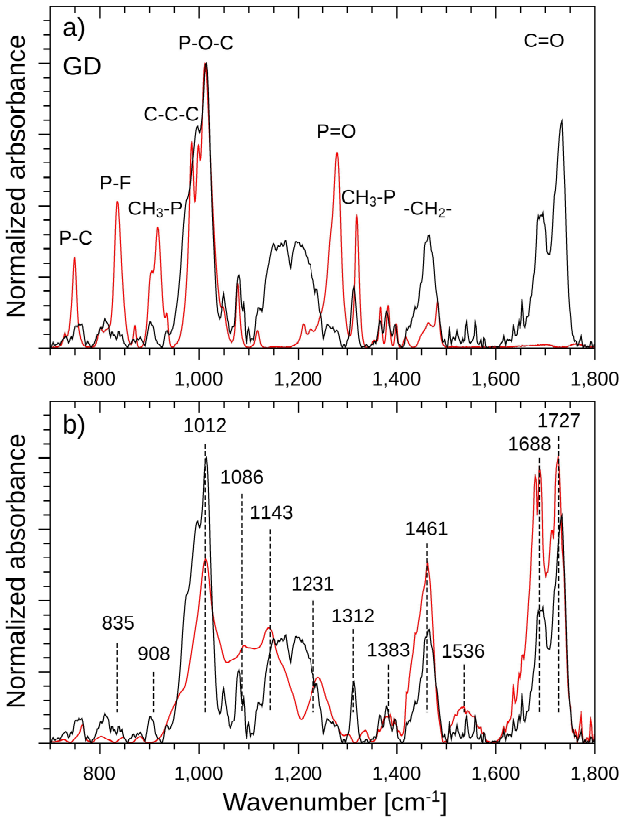

FIG. 8: Normalized ATR-FTIR spectra. The black spectrum in a) and b) is the same, namely from soman contaminated paint system A. The red spectrum in a) originates from neat soman and the red one in b) corresponds to clean paint system A.

Even though the dominating peaks originate from the substrate, certain important differences can be pointed out when comparing the (de)contaminated paint systems with the reference spectra. First of all, the peak around 1012 cm^{-1} for the paint has been enhanced relative C=O bands around 1700 cm^{-1} on the (de)contaminated surfaces (Figures 7b and 8b), which strongly indicates additional signal contribution from GB and GD residues containing C-O-P vibrations. Moreover, for soman, this peak is broadened with a shoulder at 998 cm^{-1}, likely originating from the C-C-C bending mode of soman. The contribution from G agents, or breakdown products, to the overall IR spectrum is further supported by the occurrence of the $\rho(CH_3\text{-P})$ double peak at 905-920 cm^{-1},

clearly visible in the (de)contaminated spectra. The peak at 835 cm^{-1} can be seen for both GB and GD exposed surfaces (but not for the clean substrate), indicating P-F vibrations in the top layer. Another vibrational mode at 1312 cm^{-1}, more evident for soman, is distinguishable from the clean paint system A signature, which most likely corresponds to δ_s(CH_3-P), although slightly downshifted from 1319 cm^{-1} for the neat agents. A similar shift has been reported for vaporized GB adsorption on TiO_2[34], and was therein interpreted as formation of the breakdown product isopropyl methylphosphonate (IMPA). In the same work, the ν(P=O) mode at 1277 cm^{-1} (1272 cm^{-1} here) for GB in liquid state was also shifted towards lower frequencies upon adsorption onto powdered TiO_2, i.e., down to 1252 cm^{-1}. Similar redshift of this mode has also been observed for, e.g., CWA simulants[44]. This particular mode (ν(P=O)) is relatively strong in the reference spectra, however, not observed for the (de)contaminated surfaces, at least not close to the corresponding peak in liquid state. Upon GB adsorption on powdered TiO_2 films, Hirakawa et al.[34] observed a diminished 1252 cm^{-1} band accompanied by an increase of a new broad band centered around 1210 cm^{-1}, interpreted as formation of IMPA. It is not unlikely that GB and GD react with water molecules to be decomposed to IMPA and pinacolyl methylphosphonate (PMPA), respectively, also in our case. In Figures 7b and 8b a substantial relative increase in the ATR-FTIR absorbance around 1210 cm^{-1} can be seen when comparing clean and CWA contaminated paint. Again, this effect is more pronounced for soman (Figure 8). Furthermore, contaminated paint system A also exhibits a small downshift of about 5-10 cm^{-1} for the bands at 1680-1740 cm^{-1}, meaning that the C=O group in the paint system is closely positioned or bound to the contaminant. Around 3000 cm^{-1}, where C-H vibrations are located, spectral shifts are also found and it is plausible they also are induced by specific interactions between CWA residues (intact or breakdown products) and the polymer environment of the paint. Again, this observation is more prominent for soman, pointing to a higher degree of interaction between soman related contaminations realtive the sarin counterparts. Overall, the IR studies suggest that GD is more strongly bound to the substrate compared to GB, which correlates well with the results obtained from depth profiling by LIBS which showed less mobility for GD (Figure 6).

Finally, from the depth profile data measured by LIBS on contaminated paint system A we also make an attempt to evaluate the diffusivity of GD into the first layer of paint system A. While the droplet still exists on the surface there is an abundant supply of molecules that may diffuse into the paint. However, as soon as the drop has evaporated, only a limited amount is accessible to further penetrate into the paint and to reach equilibrium. Looking at GD, the liquid layer vanished

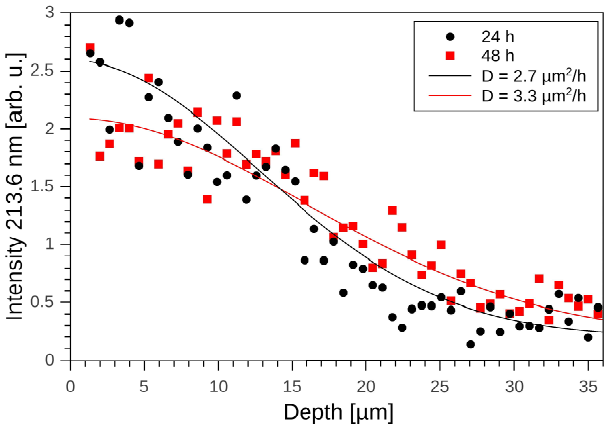

FIG. 9: Intensity of the P (213.6 nm) emission line as function of depth. Paint system A contaminated by GD after 24 and 48 hours. Solid lines represent best fit of the diffusion constant, D, using eq.(1).

after less that an hour. Even though the diffusion already started during this time (see Figure 6), we apply Fick's second law and approximate the diffusion conditions (at times $\gg$1 hour) by the thin film scenario, i.e., that all the agent molecules are at the surface ($x = 0$) at time $t = 0$ and that the diffusivity, D, is constant[45,46]. Furthermore, by assuming that the measured P line intensity, $I(x,t)$, is proportional to the concentration of agent molecules in the single shot ablated volume (or the projected average number of molecules/unit area of each "disc" of material removed), the solution of the diffusion equation can be expressed as:

$$I(x,t) = \frac{I_M}{\sqrt{\pi D t}} \exp\left(-\frac{x^2}{4Dt}\right) + B, \quad (1)$$

where I_M is proportional to the total amout of agent molecules per unit area and B the average background level.

By fitting eq.(1) to the intensity data taken at two different times (24 and 48 h) after GD droplet deposition on paint system A, we obtain approximately the same diffusivity ($D \approx 3$ μm^2/h), see Figure 9. Here, B was set to 0.2 (average of background signal, see Figure 6) and I_M = 38. Note that the intensity obtained by the first laser pulse was omitted for the fit.

The quite good fitting results, even though rather crude approximations were made, suggest that the LIBS method can be useful to obtain approximative values of D, at least in the particular model system described above. However, further studies in this direction would be needed to better confirm these preliminary results, preferably in combination with numerically solved diffusion models, which allows for better description of the current (non-stationary) initial conditions.

IV. CONCLUSIONS

The LIBS technique showed promising results with applications related to detection of contamination of CWA and simulants on and inside different substrates, and also for evaluating decontamination procedures. It also looks promising to monitor the diffusion properties of contaminants into certain materials. This initial study of the behavior of nerve agents and simulants on the different substrates suggests, as expected, that no (or below the detection limit) penetration could be observed for Si wafers and the CARC paints. However, for the cover paint in system A a diffusion into the paint was clearly observed.

ATR-FTIR spectroscopy was successfully applied to verify CWA residues bound in the polymer based paint system A. Importantly, several spectral features can be related to phosphorous (P-F, C-O-P and CH_3-P). The ATR-FTIR results also indicate the presence of the breakdown product IMPA. Soman seems to interact stronger with the paint system A compared to sarin, as indicated by both the LIBS and ATR-FTIR studies.

Furthermore, decontamination of these chemicals from Si wafer and paint system B is likely an easy task, whereas it might be more problematic for the topmost layer of paint system A. Future studies of improved spectroscopic methods seem warranted as well as expanding the contaminated model systems to include, e.g., skin, protective equipment, filters, etc., as substrates. For LIBS, it would also be of great interest to analyze more CWA indicative elements, such as S, F, and Cl.

Acknowledgments

This work was funded by the Swedish Department of Defence, Project no. 410-A403215.

---

* Electronic address: lars.landstrom@foi.se

[1] U. Ivarsson, H. Nilsson, and J. Santesson, eds., *A FOA briefing book on chemical weapons: threat, effects and protection* (Försvarets Forskningsanstalt, Sundbyberg, Sweden, 1992).

[2] Y. C. Yang, J. A. Baker, and J. R. Ward, Chem. Rev. **92**, 1729 (1992).

[3] B. Singh, G. K. Prasad, K. S. Pandey, R. K. Danikhel, and R. Vijayaraghavan, Def. Sci. J. **60**, 428 (2010).

[4] K. Kim, O. G. Tsay, D. A. Atwood, and D. G. Churchill, Chem. Rev. **111**, 5345 (2011).

[5] S. Eto, T. Matsuo, T. Matsumura, T. Fujii, and M. Y. Tanaka, Spectrochim. Acta B **101**, 245 (2014).

[6] E. Gazi and S. J. Mitchell, J. Coat. Technol. Res. **9**, 735 (2012).

[7] K. Amponsah-Manager, N. Omenetto, B. W. Smith, I. B. Gornushkin, and J. D. Winefordner, J. Anal. At. Spectrom. **20**, 544 (2005).

[8] M. P. Mateo, G. Nicolas, V. Pinon, and A. Yanez, Surf. Interface Anal. **38**, 941 (2006).

[9] A. W. Miziolek, V. Palleschi, and I. Schechter, eds., *Laser Induced Breakdown Spectroscopy* (Cambridge University Press, Cambridge, 2006).

[10] D. W. Hahn and N. Omenetto, Appl. Spectrosc. **64**, 335A (2010).

[11] D. W. Hahn and N. Omenetto, Appl. Spectrosc. **66**, 347 (2011).

[12] D. C. S. Beddows and H. H. Telle, Spectrochim. Acta, Part B **60**, 1040 (2005).

[13] D. W. Hahn and N. Omenetto, Appl. Spectrosc. **64**, 335 (2010).

[14] S. Morel, N. Leone, P. Adam, and J. Amouroux, Appl. Opt. **42**, 6184 (2003).

[15] D. W. Hahn and N. Omenetto, Appl. Spectrosc. **66**, 347 (2012).

[16] P. V. Maravelaki, V. Zafiropoulos, V. Kilikoglou, M. Kalaitzaki, and C. Fotakis, Spectrochim. Acta, Part B **56**, 707 (1997).

[17] M. O. Vieitez, J. Hedberg, O. Launila, and L. E. Berg, Spectrochim. Acta, Part B **60**, 920 (2005).

[18] S. Rosenwasser, G. Asimellis, B. Bromley, R. Hazlett, J. Martin, and A. Zigler, Spectrochim. Acta, Part B **56**, 707 (2001).

[19] T. Kim, B. T. Nguyen, and V. Minassian, J. Coat. Technol. Res. **4**, 241 (2007).

[20] J. L. Gottfried, D. L. F. C., C. A. Munson, and A. W. Miziolek, Appl. Spectrosc. **62**, 353 (2008).

[21] G. A. Lithgow and S. G. Buckley, Appl. Phys. Lett. **87**, 011501 (2005).

[22] D. L., P. Adam, and J. Amouroux, Appl. Spectrosc. **52**, 1321 (1998).

[23] F. C. DeLucia, A. C. Samuels, R. S. Harmon, R. A. Walters, K. L. McNesby, A. LaPointe, R. J. Winkel, and A. W. Miziolek, IEEE Sens. J. **5**, 681 (2005).

[24] T. Tjärnhage, P.-Å. Gradmark, A. Larsson, A. Mohammed, L. Landström, E. Sagerfors, P. Jonsson, F. Kullander, and M. Andersson, Opt. Commun. **296**, 106 (2013).

[25] L. Landström, A. Larsson, P.-Å. Gradmark, L. Örebrand, P. O. Andersson, P. Wästerby, and T. Tjärnhage, Proc. SPIE **9073**, 907312 (2014).

[26] A. Larsson, H. Andersson, and L. Landström, J. Anal. At. Spectrom. (2015).

[27] J. L. Gottfried, F. C. De Lucia, C. A. Munson, and M. A. W., J. Anal. At. Spectrom. **23**, 205 (2008).

[28] P. Lucena, A. Dona, L. M. Tobaria, and J. J. Laserna, Spectrochim. Acta Part B **66**, 12 (2011).

[29] F. R. Doucet, G. Lithgow, R. Kosierb, P. Bouchard, and M. Sabsabi, J. Anal. At. Spectrom. **26**, 536

(2011).

[30] D. A. Woods and C. D. Bain, Soft Matter **10**, 1071 (2014).

[31] G. Asimellis, A. Giannoudakos, and M. Kompitsas, Spectrochimica Acta Part B **61**, 1253 (2006).

[32] L. St-Onge, E. Kwong, M. Sabsabi, and E. B. Vadas, Spectrochim. Acta Part B **57**, 1131 (2002).

[33] C. M. Li, Z. M. Zou, X. Y. Yang, Z. Q. Hao, L. B. Guo, X. Y. Li, Y. F. Lu, and X. Y. Zeng, J. Anal. At. Spectrom. (2014).

[34] T. Hirakawa, K. Sato, A. Komano, S. Kishi, C. K. Nishimoto, N. Mera, M. Kugishima, T. Sano, H. Ichinose, N. Negishi, et al., The Journal of Physical Chemistry C **114**, 2305 (2010).

[35] D. M. Crawford and J. A. Escarsega, Thermochimica Acta **357-358**, 161 (2000).

[36] A. Kramida, Y. Ralchenko, J. Reader, and NIST ASD Team, NIST Atomic Spectra Database (version 5.1) (2014).

[37] J. Bailey, S. A. McHugo, H. Hieslmair, and E. R. Weber, J. Electron. Mater. **25**, 1417 (1996).

[38] E. D. Davis, W. O. Gordon, A. R. Wilmsmeyer, D. Troya, and J. R. Morris, The Journal of Physical Chemistry Letters **5**, 1393 (2014).

[39] S. W. Sharpe, T. J. Johnson, P. M. Chu, J. Kleimeyer, and B. Rowland, Proc. SPIE **5085**, 19 (2003).

[40] A. R. Wilmsmeyer, W. O. Gordon, E. D. Davis, D. Troya, B. A. Mantooth, T. A. Lalain, and J. R. Morris, The Journal of Physical Chemistry C **117**, 15685 (2013).

[41] C. Duce, V. Della Porta, M. R. Tiné, A. Spepi, L. Ghezzi, M. P. Colombini, and E. Bramanti, Spectrochimica Acta Part A: Molecular and Biomolecular Spectroscopy **130**, 214 (2014).

[42] J. Lv, J. Feng, Y. Liu, Z. Wang, M. Zhao, and R. Shi, Analytical Letters **45**, 1079 (2012).

[43] Z. O. Oyman, W. Ming, and R. van der Linde, Progress in Organic Coatings **48**, 80 (2003).

[44] A. Mattsson, C. Lejon, V. Stengl, S. Bakardjieva, F. Oplustil, P. O. Andersson, and L. Österlund, Applied Catalysis B: Environmental **92**, 401 (2009).

[45] A. Fick, Annalen der Physik **170**, 59 (1855).

[46] H. Mehrer, ed., *Diffusion in Solids: Fundamentals, Methods, Materials, Diffusion-Controlled Processes* (Springer-Verlag, Berlin Heidelberg, 2007).